

Using polarimetric C-Band data to discriminate wetland vegetation in the Lower Paraná River floodplain: assesment of a supervised object-based Random Forests classifier

Natalia Soledad Morandeira^{1,2}
Luiz Felipe de Almeida Furtado³

¹ Instituto de Investigaciones en Ingeniería Ambiental (3iA)
Universidad Nacional de San Martín (UNSAM)
Campus Miguelete, General San Martín, Buenos Aires, Argentina
nmorandeira@unsam.edu.ar

² Consejo Nacional de Investigaciones Científicas y Tecnológicas (CONICET)
Argentina

³ Instituto Nacional de Pesquisas Espaciais – INPE
CEP 12227-010 – São José dos Campos - SP, Brasil
furtadosere@gmail.com

Abstract. The Lower Paraná River floodplain wetlands are dominated by herbaceous communities. Dominant macrophyte species have been classified in Plant Functional Types, summarizing their main structural and functional features and their expected responses to the environment. In a previous work, a polarimetric RADARSAT-2 C-Band scene was classified with an unsupervised per-pixel approach on the coherence matrix (a progressive Wishart H/α classifier), but a relatively low global accuracy (58.2%) and Kappa index (50.4%) were obtained. In this work, we assessed a supervised object-based Random Forests classifier on the same scene. Based in previous works in other areas, we expected a higher accuracy for the Random Forests classifier than for the Wishart one. However, we obtained a even lower global accuracy (55.2%) and Kappa index (40.6%). Also, most of the areas were assigned to Plant Functional Type A (corresponding to bulrush marshes). We compared the classifiers and discuss possible reasons for the lower accuracy of the object based classifier. Our results suggest that most of the errors can be caused by the high similarities between the Plant Functional Type classes and between short grasses and Bare Soil. Other possible explanation of the low accuracy of the Random Forests classifier is that it does not follow the statistical distribution of the polarimetric data.

Keywords: classification, macrophytes, RADARSAT-2

Palavras chave: classificação, macrófitas, RADARSAT-2

1. Introduction

The largest wetlands of South America are associated with the floodplains of the Amazonas, Orinoco and Paraná-Paraguay Rivers (JUNK, 2012). Due to their large extensions and their restricted accessibility, remote sensing is a valuable tool for assessing the state and dynamics of floodplain wetlands. In the last decades, Synthetic Aperture Radar (SAR) data have been noted as a promising tool to discriminate wetland vegetation types, mainly due to the ability to detect water below the vegetation (HENDERSON; LEWIS, 2008). Polarimetric SAR data (containing complex information on amplitude and phase in HH, HV and VV) are only recently used: the first polarimetric satellital system has been launched in 2006 (ALOS/PALSAR-1). Thus, the experience on the extraction of polarimetric information and on polarimetric classifications is scarce in natural environments, and particularly in wetland ecosystems (Touzi, Deschamps, and Rother 2009).

Classification procedures on polarimetric SAR data have been performed both with per-pixel and with object-based approaches, and both with unsupervised and supervised schemes. Also, some classifiers use decompositions on the covariance or coherence matrixes (PATEL; SRIVASTAVA; NAVALGUND, 2009; Rúbio Sartori et al., 2011). In the Lower Paraná River Delta, an area of herbaceous wetlands has been classified with a polarimetric RADARSAT-2 C-Band scene (MORANDEIRA, 2014), through an unsupervised per-pixel approach (a progressive Wishart H/α classification, see details in Section 2.5). The accuracy obtained in that product was relatively low (58.2%), but improved the previous vegetation maps for the area. Also, the information classes were defined in functional terms (Plant Functional Types (PFT)) (DÍAZ; CABIDO, 2001), giving valuable ecological information of the floodplain as well as the ability to predict the vegetation responses to disturbances, anthropic impacts or global change.

Object-based classifications have shown higher accuracy than per-pixel approaches in several works which aimed to map vegetation types (e.g., Rúbio Sartori et al. (2011)). In this work we performed a supervised object-based classification (Blackshe 2014) on the RADARSAT-2 scene mentioned above. We hypothesized that this different approach will improve the accuracy of the unsupervised Wishart classifier. Our propose was to segment the scene in objects. Next, a machine learning classifier named Random Forests (Breiman 2001) was used to classify the objects, based in given information about “training samplings”.

2. Methods

2.1. Study area

The study was conducted in the Lower Paraná River floodplain next to Ramallo city (Figure 1), which is subject to the flood pulse of the Paraná River. The climate is temperate humid. The area is relatively flat and is dominated by herbaceous communities distributed with a zonation pattern. Forest patches cover ca. 1.5% of the study area (estimated from Enrique (2009)). The main commercial activity is cattle, which depends on the natural herbaceous vegetation of the area. Fishery and apiculture are also important commercial activities.

2.2. Field sampling and information classes

Vegetation sampling was conducted during summers 2010-2011 and 2011-2012 in 42 georeferenced sampling sites distributed along the study area. Based in three Braun-Blanquet abundance-cover censuses per site Mueller-Dombois e Ellenberg (1974) and in trait measurements, we identified the dominant plant functional types (PFT). Species were assigned to PFT through multivariate clustering and their functions were deduced from trait values (MORANDEIRA, 2014). We also recorded the location of three sites with bare soil (cattle corrals or areas with high cattle transit) and of ten sites of open water (shallow lakes and rivers). Minimum aboveground green biomass is similar within PFT (100 to 290 g.m⁻²). Maximum biomass ranges between 620 g.m⁻² and 3340 g.m⁻² and can be ordered as follows: PFT D < B < C < A < E. The five dominant PFT can be described following Morandeira (2014):

PFT A. Equisetoid herbs (*Schoenoplectus californicus*, *Cyperus giganteus*). Plants are characterized by vertical photosynthetic stems of 140 to 250 cm height. Strong competitors growing in low topographic positions, in generally flooded sites.

PFT B. Short broadleaf marshes (*Sagittaria montevidensis*, *Eclipta prostrata*, *Enydra anagallis*). Plants are generally shorter than 80 cm and have few leaves with high leaf areas. Ruderal plants growing in low topographic positions, in generally flooded or soil-saturated sites with high soil fertility.

PFT C. Tall broadleaf marshes (*Baccharis salicifolia*, *Conyza bonariensis*, *Polygonum acuminatum*, *Ludwigia* cf. *peruviana*). Plants between 150 and 250 cm height, usually with

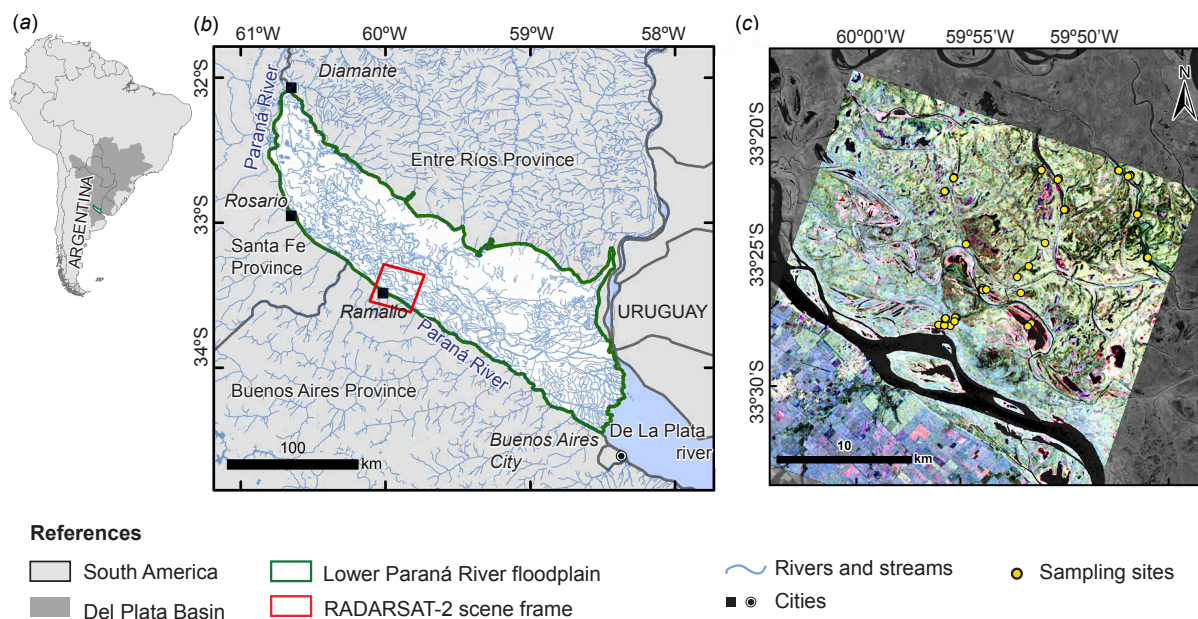


Figure 1: Study Area. (a) Location of the Lower Paraná River floodplain in South America and in the Del Plata basin. (b) Lower Paraná River floodplain (also known as Paraná River Delta), from Diamante city to the De La Plata River. (c) RGB Pauli representation of the RADARSAT-2 scene of date 01/30/2011: HH+VV (R), HH-VV (G), HV (B)

abundant leaves and ramified stems. Ruderal plants or medium competitors, growing in high (in generally non-flooded nor saturated sites) or in low topographic positions (in flooded sites).

PFT D. Short grasslands and grass marshes (*Cynodon dactylon*, *Paspalum vaginatum*, *Echinochloa helodes*). Plants shorter than 50 cm in height, with few leaves. Stress-tolerant species (both for salinity or dry conditions) or ruderal species, growing in high or medium topographic positions.

PFT E. Tall grasslands and grass marshes (*Panicum elephantipes*, *Hymenachne pernambucense*, *Echinochloa crus-gallis*, *Bolboschoenus robustus*, *Leptochloa fusca*.). Ruderal plants growing in low or medium topographic positions.

Using the information of the field sampling points as well as optic imagery (Landsat 5 TM, SPOT 5) from close dates and Google Earth interpretation, we generated 144 sampling polygons. In the next steps, half of them were used to train the supervised classifier and the other half were used to evaluate the product accuracy.

2.3. Preprocessing of the RADARSAT-2 scene

A Fine Quad-Pol RS2 scene was acquired on 01-30-2011 (Single Look Complex product). The beam was FQ24, with a near incidence angle of 42.8° and a far incidence angle of 44.1°. The scene covered 25 x 25 km and its resolution was of 5.2 m x 7.6 m, getting to a final pixel resolution of 12.5 m. At the scene acquisition date, the hydrometric level in the Paraná River was low and far below the level for which water begins entering the floodplain. Pre-processing was done with PolSARpro (European Space Agency, 2011). The T3 coherence matrix and the C3 covariance matrix were geocodified with MapReady (Alaska Satellite Facility, 2013), without applying a terrain correction. The scene was filtered with a 7x7 adaptive Lee filter (LEE, 1986). Backscattering coefficients in HH, HV and VV were extracted and transformed from intensity to decibels (dB).

2.4. Supervised Random Forests GEOBIA classifier

We generated a stack with the nine components of the T3 matrix: the intensity (expressed in dB) of the diagonals (T11, T22 and T33) and both the intensity (expressed in dB) and phase of T12, T13, and T23. This stack was segmented using eCognition, restricted by the shape of the training sample polygons. For each resultant object, mean values of each of the T3 components were assigned. Training samples were associated to the corresponding object, so that a machine learning algorithm could be initialized. We computed a Random Forests classification (RF from now on) (BREIMAN, 2001) in R Project, using the script *RFClassifier* developed by Jefferson Ferreira-Ferreira and Thiago Sanna Freire Silva. Thus, we obtained a classified vectorial map. We generated 5000 random trees and 5 number of variables to be randomly sampled as candidates at each split in each tree. The level of importance of each variable for determining each split in each tree was inspected through the mean decrease in Gini values. The mean decrease in Gini coefficient is a measure of how each variable contributes to the homogeneity of the nodes in the resulting random forest. Variables that are more important in the classification improve class discrimination.

The accuracy of the final product was evaluated by comparing the classified polygons with the evaluation sampling polygons. The global accuracy, the omission and commission errors and the Kappa index Congalton (1991) were computed.

2.5. Comparison with an unsupervised H/ α Wishart product

We compared the final map product and the accuracy with a previously performed map on the same polarimetric scene (MORANDEIRA, 2014). That map has been performed with an unsupervised per-pixel approach. The first step was to obtain the entropy (H), mean alpha angle (α) and the anisotropy (A) by decomposing the T3 matrix (CLOUDE; POTTIER, 1997). Next, a Wishart complex classifier was initialized from the centroids of a H/ α segmentation, thus obtaining 8 classes. For classes with mean H > 0.9, a progressive classification using A was performed. The 8 resulting classes were then assigned to the seven information classes described above (water, bare soil and PFT) based on predictions on their expected H and α values. Also, a class with few number of pixels, low H and very high α was assigned to ships and ports (dihedral reflection) and excluded from further analysis. The accuracy of this classification was evaluated with a per-pixel analyses on 55 field sampling sites (42 of PFT, 3 of bare soil and 10 of water).

3. Results and discussion

3.1. Supervised Random Forest classification product

The statistics of the sampling polygons denote that some of the classes defined above are difficult to discriminate with the T3 components (Figure 2). Phase differences were similar within all the vegetation types. Consistently, the most important variables in the RF model (i.e, those with the highest mean decrease in Gini values) were the diagonals of the T3 matrix expressed in dB (Figure 3). In particular, T22 had the highest contribution to nodes homogeneity. Since T22 component is related to the double-bounce scatter contribution to the backscattering coefficient, its importance in the model might be caused by the discrimination of PFT A. Grings et al. (2005) have modelled the presence of double-bounce scatter in C-Band for flooded sites with *Schoenoplectus californicus*, and that species is the dominant one in PFT A. Also, Bare Soil and PFT D showed lower T22 values than PFTs B, C and D; and Water showed very low T22 values (Figure 2). The contribution of T11 (surface scatter) and of T33 (volume scatter) was lower than the contribution of T22. However, note that PFT D had low T11 values, and both PFT D and Bare Soil had low T33 values (Figure 2).

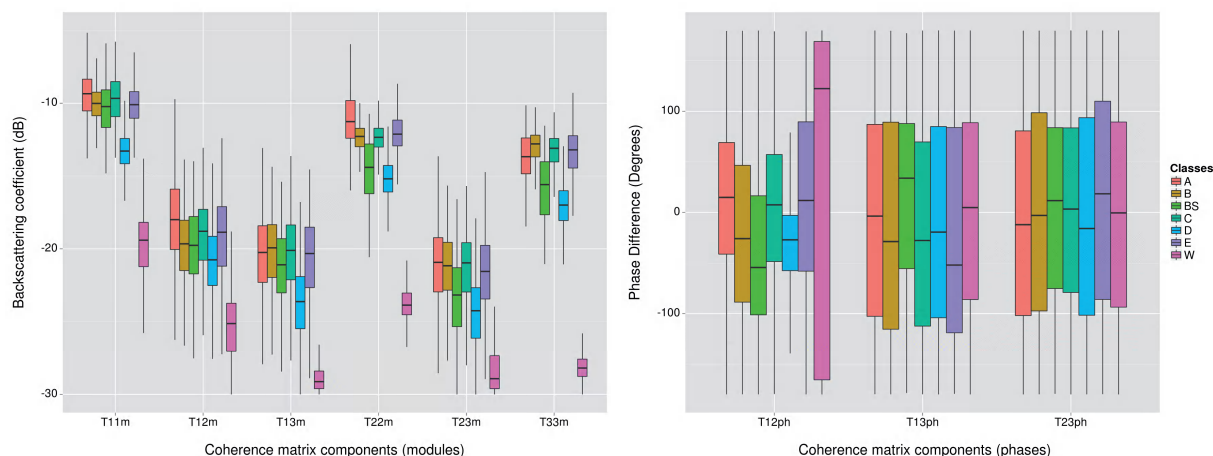


Figure 2: Components of the coherence matrix for the sampling polygons (n = 144) of each information class.

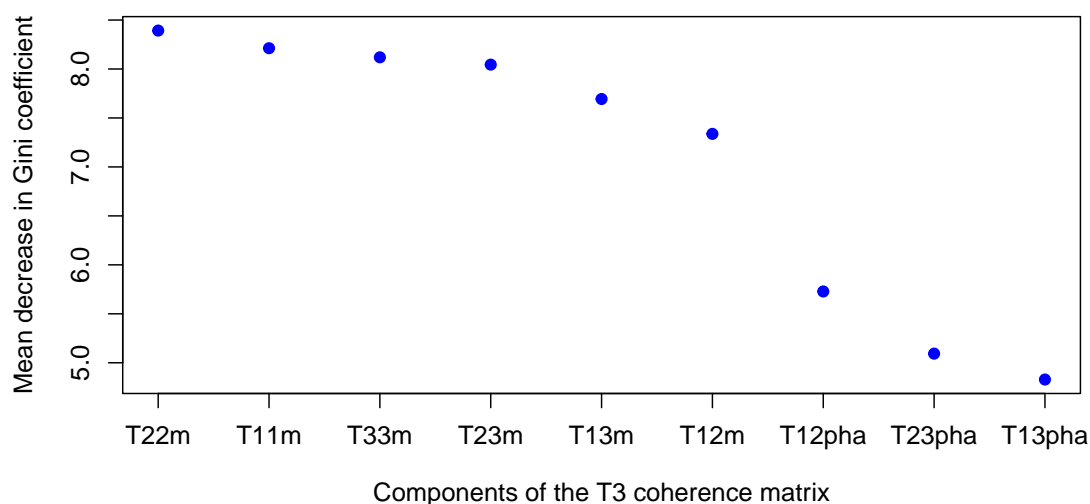


Figure 3: Conditional importance of the variables included in the model. A higher mean decrease in Gini indicates that the variable has a higher contribution to the homogeneity of the nodes in the resulting random forest.

The zonation pattern of vegetation was well identified by the classifier (Figure 4). However, the relative proportions of the PFT information classes fairly contrast with our field observations and our knowledge of the study area. For example, while the most abundant class in the map was PFT A (35% of the total area), in the field PFT is restricted to just some of the low topographic positions in the middle of the islands, whereas broad-leaf herbs (particularly those from PFT C) are dominant, followed by tall grasslands from PFT E.

The global accuracy of the RF product was 55.9% and the Kappa index was 40.6%. Classes PFT B, PFT E and Bare soil had maximum omission and commission errors. PFT B was mainly confused with E, whereas E was confused with A, B and C. Besides, Bare Soil was mainly confused with PFT E.

3.2. Comparison between classification products

The RF and the Wishart classifications were coincident in a 34.6%. The main dissimilarities arose in class E, to which less than 0.01% of the pixels were assigned in the RF product. This

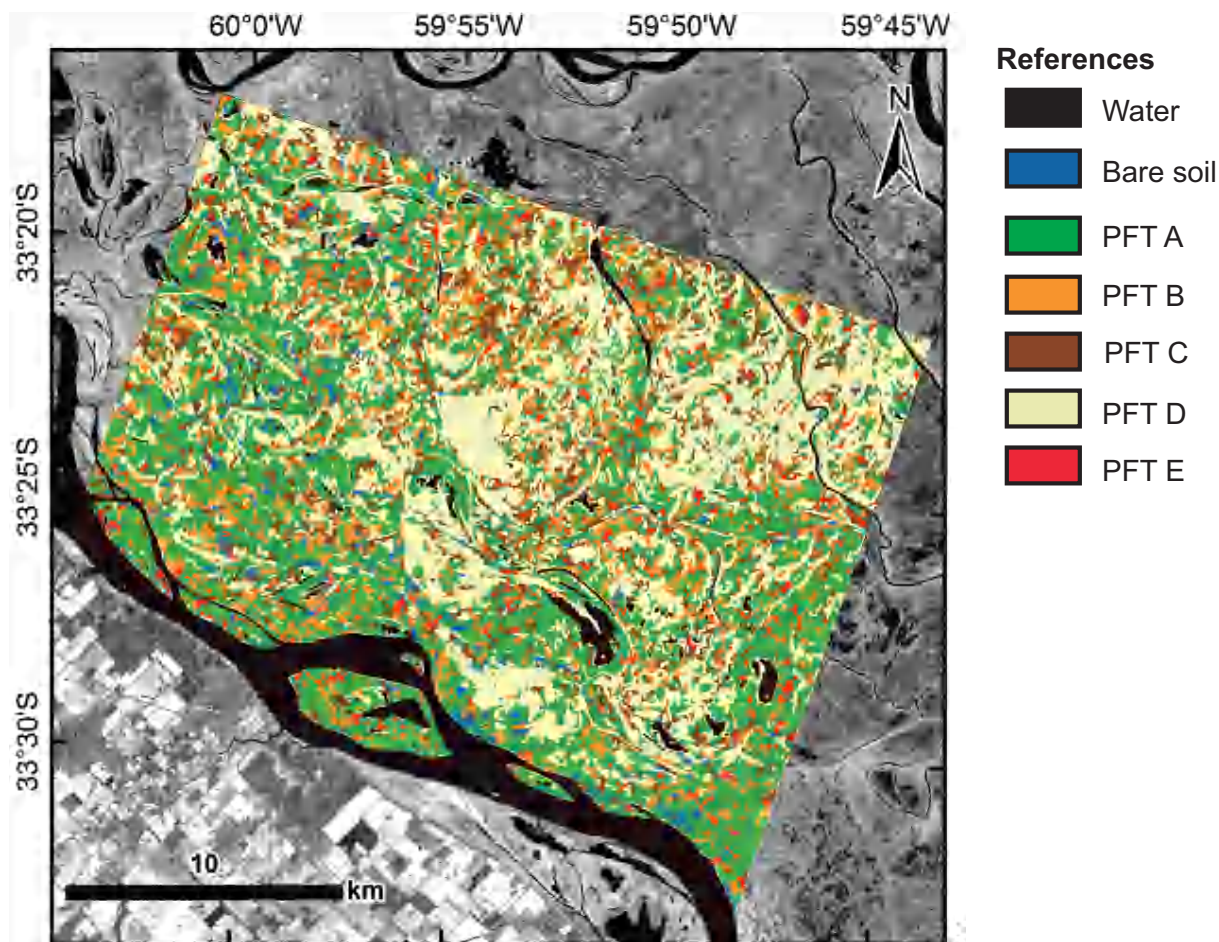


Figure 4: Supervised Random Forest GEOBIA classification product of Plant Functional Types areas, performed on a polarimetric RADARSAT-2 scene (date: 01-30-2011). For more details on class features and mapping procedure, see the text. The background image is a grayscale display of a Landsat 5 TM scene.

result contrasts with the spatial coverage of Class E. Class A has a much higher spatial coverage in the RF product than in the Wishart one (35% vs. 5.5% of the total area, respectively). Conversely, class C has a much lower spatial coverage in the RF product than in the Wishart one (8.9% vs. 33.8%). The global accuracy and the Kappa index were slightly higher in the Wishart product than in the RF product (Table 1). When excluding the water class for the accuracy assessment, the Kappa indexes of both products significantly differed (as indicated by their 0.95 confidence interval) and the Wishart classification was preferred.

4. Conclusions

The supervised object-based RF classifier on a C-Band polarimetric scene assessed in this work led to a low accuracy product. Most of the areas were assigned to PFT A (ruderal equisetoid species, dominant in bulrush marshes) and not to the most abundant PFTs (C or E). This may be due to the high similarities between the PFT classes and between PFT D and Bare Soil. Other possible explanation of the low accuracy of the RF classifier is that it does not follow the statistical distribution of the polarimetric data. An unsupervised H/α Wishart classification on the same polarimetric scene has a higher accuracy than the RF classification, specially when comparing the accuracy of the non-Water classes. This suggests that small differences between classes are well exploited by the Wishart classifier and its iteration procedure. In

Table 1: Comparison between the accuracy of the Random Forest product and the accuracy of the Wishart H/ α classifier

Accuracy (%)	Random Forests		Wishart H/ α	
	With water	Without water	With water	Without water
Global accuracy	55.9	35.2	58.2	48.9
Kappa index	40.6	18.8	50.4	41.8
0.95 confidence interval	29.8 – 51.5	6.3 – 31.3	35.9 – 65.9	23.3 – 60.2
% of maximum Kappa	58.2	31.3	55.2	44.3
Mean omission error	62.1	71.4	38.8	45.3
Mean commission error	70.35	82.08	41.4	44.5
<i>Omission error per class</i>				
PTF A		28.6		50.0
PFT B		100.0		57.1
PFT C		87.5		37.5
PFT D		12.5		70.0
PFT E		100.0		57.1
Bare soil		100.0		0.0
Water		6.1		0.0
<i>Commission error per class</i>				
PTF A		62.5		44.4
PFT B		100.0		40.0
PFT C		81.8		37.5
PFT D		48.1		70.0
PFT E		100.0		50.0
Bare soil		100.0		25.0
Water		0.0		23.1

that classification scheme, the assignment of the spectral classes to the desired information classes was defined by our predictions about the expected H and α values per class. The supervised object-based RF approach assessed in this work can be influenced by the definition of the training areas, specially when extending the field sampling points ($n = 55$) to a higher number of training and assessment polygons ($n = 144$). Consistently, a supervised Wishart classifier performed in this scene also led to very low global accuracy (results not shown), since it maximized the discrimination of the training areas and not the separability of the spectral classes in the full scene. To better understand whether the low accuracy is due to the object-based approach or due to the supervised scheme, a comparison between supervised and non-supervised object-based approaches would be desirable. Future works should evaluate whether a better product is achieved by including geographic information of the objects (shape, area, proximity, within-object features such as texture, etc.).

Acknowledgments: RS2 imagery was acquired through a project with the Canadian Space Agency. This work was funded by Comisión Nacional de Actividades Espaciales (CONAE, Argentina: AO SAOCOM N° 22) and by Agencia Nacional de Promoción Científica y Técnica (PICTO-CIN I-22, PI Patricia Kandus). We thank Juan Nazar and Bello family for logistic help during field sampling. Several people collaborated during field work: M. Borro, M. Schoo,

S. Varela, M. R. Derguy, M. S. Erario, A. Falthausner, M. Lanfutti and V. Pacotti. The Wishart classification here discussed was carried out by N. Morandeira, F. Grings, C. Facchinetti and P. Kandus.

References

- Alaska Satellite Facility. *ASF Map Ready v. 3.0.6*. 2013. Disponível em: <<https://www.asf.alaska.edu/data-tools/mapready/>>.
- BREIMAN, L. E. O. Random Forests. *Machine Learning*, v. 45, p. 5–32, 2001. ISSN 0885-6125.
- CLOUDE, S. R.; POTTIER, E. An entropy based classification scheme for land applications of polarimetric SAR. *IEEE Transactions on Geoscience and Remote Sensing*, v. 35, n. 1, p. 68–78, 1997. ISSN 01962892. Disponível em: <<http://ieeexplore.ieee.org/lpdocs/epic03/wrapper.htm?arnumber=551935>>.
- CONGALTON, R. G. A review of assessing the accuracy of classifications of remotely sensed data. *Remote Sensing of Environment*, v. 46, p. 35–46, 1991.
- DÍAZ, S.; CABIDO, M. Vive la différence: plant functional diversity matters to ecosystem processes. *Trends in Ecology and Evolution*, v. 16, n. 11, p. 646–655, 2001. Disponível em: <<http://www.sciencedirect.com/science/article/pii/S0169534701022832>>.
- ENRIQUE, C. *Relevamiento y caracterización florística y espectral de los bosques de la Región del Delta del Paraná a partir de imágenes satelitales*. 93 p. Tese (Degree Thesis in Biological Sciences. Facultad de Ciencias Exactas y Naturales, Universidad de Buenos Aires.), Buenos Aires, 2009.
- European Space Agency. *PolSARpro. V. 4.2*. 2011. Disponível em: <<http://earth.eo.esa.int/polsarpro/>>.
- GRINGS, F. et al. Modeling temporal evolution of junco marshes radar signatures. *Geoscience and Remote Sensing, IEEE Transactions on*, v. 43, n. 10, p. 2238–2245, Oct 2005. ISSN 0196-2892.
- HENDERSON, F. M.; LEWIS, A. J. Radar detection of wetland ecosystems: a review. *International Journal of Remote Sensing*, v. 29, n. 20, p. 5809–5835, out. 2008. ISSN 0143-1161.
- JUNK, W. J. Current state of knowledge regarding South America wetlands and their future under global climate change. *Aquatic Sciences*, v. 75, n. 1, p. 113–131, mar. 2012. ISSN 1015-1621. Disponível em: <<http://link.springer.com/10.1007/s00027-012-0253-8>>.
- LEE, J.-S. Speckle suppression and analysis for Synthetic Aperture Radar images. *Optical Engineering*, v. 25, n. 5, p. 255636, 1986.
- MORANDEIRA, N. S. *Tipos funcionales de plantas en humedales de la planicie de inundación del Bajo Río Paraná (Entre Ríos , Argentina) y su observación con datos polarimétricos de radar*. 278 p. Tese (Doutorado), 2014. Disponível em: <http://digital.bl.fcen.uba.ar/Download/Tesis/Tesis_5490_Morandeira.pdf>.
- MUELLER-DOMBOIS, D.; ELLENBERG, H. *Aims and methods of vegetation ecology*. New York: John Wiley, 1974. 547 p.
- PATEL, P.; SRIVASTAVA, H. S.; NAVALGUND, R. R. Use of synthetic aperture radar polarimetry to characterize wetland targets of Keoladeo National Park, Bharatpur, India. *Current Science*, v. 97, n. 4, p. 529–537, 2009.
- Rúbio Sartori, L. et al. Mapping macrophyte species in the Amazon floodplain wetlands using fully polarimetric ALOS/PALSAR data. *IEEE Transactions on Geoscience and Remote Sensing*, v. 49, n. 12, p. 4717–4728, 2011.